Journal of Zhejiang University-SCIENCE A (Applied Physics & Engineering)
ISSN 1673-565X (Print); ISSN 1862-1775 (Online)
www.jzus.zju.edu.cn; www.springerlink.com
E-mail: jzus@zju.edu.cn

A strength degradation model of saturated soft clay and its application in caisson breakwater*

Zhen YAN[†1,2,3], Yuan-zhan WANG[3], Zhong-xuan YANG[†‡2], Zhong XIAO[3], Kun PAN[2]

[1]*Tianjin Research Institute for Water Transport Engineering, Ministry of Transport, Tianjin 300456, China*

[2]*Research Center of Coastal and Urban Geotechnical Engineering, Engineering Research Center of Urban Underground Development of Zhejiang Province, Zhejiang University, Hangzhou 310058, China*

[3]*School of Civil Engineering, Tianjin University, Tianjin 300072, China*

[†]E-mail: yanzhen19890206@163.com; zxyang@zju.edu.cn

Received Aug. 30, 2017; Revision accepted Jan. 25, 2018; Crosschecked July 6, 2018

Abstract: In this paper we propose a degradation model to describe the damage-dependent behavior of saturated soft clay under cyclic loading, which is then applied to the analysis of a caisson breakwater. The degree of damage and remolding of soft clay is quantified by a damage parameter related to the accumulated plastic deviatoric strain. Through the correlation between the maximum pore pressure and the undrained strength of soft clay, we obtain a damage-dependent degradation model that employs the post-cyclic undrained strength degradation coefficient in terms of the cyclic stress ratio and the number of cycles. Based on the Tresca yield criterion, the degradation model of undrained strength of soft clay is numerically implemented in the user interface USDFLD of ABAQUS. The performance of this model is verified by a comparison between numerical results (finite element method) and experimental data (cyclic triaxial test). The model is applied to the numerical simulation of a caisson breakwater resting on a partially sand-filled soft clay seabed under cyclic wave loading. The cyclic stress distribution, pore pressure development, and strength degradation of the seabed soil are presented to illustrate the applicability and efficiency of the model in the analysis of the interaction between offshore structures and soft ground.

Key words: Saturated soft clay; Undrained strength; Degradation model; Damage dependency; Numerical simulation
https://doi.org/10.1631/jzus.A1700461 **CLC number:** TU473

1 Introduction

As a typical offshore structure, a caisson breakwater is always subject to wave-induced cyclic loading (Oumeraci, 1994; Ulker et al., 2010), which is thus transferred to the soft clay grounds on which the superstructures are built. Under long-term cyclic loading conditions such as ocean wave loading, the undrained strength of clay may be gradually degraded (Andersen and Lauritzsen, 1988; Yasuhara, 1994; Chen and Randolph, 2007; Liyanapathirana, 2009; Mortezaie and Vucetic, 2013; Cai et al., 2017; Guo et al., 2018). This has been attributed to the continuous destruction of the soil fabric and the development of excess pore pressure under undrained conditions (Kudella et al., 2006; Mortezaie and Vucetic, 2013; Zhou et al., 2014), resulting in the significant loss of the bearing capacity of foundations and thus the reduction of the stability of superstructures. For example, during the construction of the guiding dike in the Yangtze Estuary, some of the caisson units sank into the soil for 1–5 m or slid about 20 m away from the original place when a strong storm attacked this area in 2002 (Yan et al., 2005). The settlement of the

‡ Corresponding author

* Project supported by the National Natural Science Foundation of China (Nos. 51479133, 51409134, and 51279128), the Fundamental Research Funds for the Central Research Institutes (Nos. TKS140210, TKS170102, and TKS170108)

ORCID: Zhen YAN, https://orcid.org/0000-0003-1366-399X

vertical caisson breakwater in the Yantai port test section, China was reported to be up to 1 m after a long period of wave loading (Yang, 2014). These cases of deterioration demonstrate that degradation of the strength of soils should be considered in the analysis of offshore engineering problems (Xiao et al., 2016).

Some constitutive models can consider the cyclic degradation of the undrained strength of soils (Lee and Oh, 1995; Allotey and El Naggar, 2008; Huang et al., 2011; Hu and Liu, 2015). However, the numerous parameters required by these models may restrict their practical application to caisson breakwaters. Gerolymos and Gazetas (2006) developed a Winkler-spring method to capture the cyclic response of caisson foundations in terms of the separation and slippage of the caisson-soil interface, the uplift of the caisson base, and the stiffness and strength degradation of soft clay. However, such a simplified soil reaction theory fails to provide any information on the transition from the elastic to the ultimate limit state of soil reaction (Karapiperis and Gerolymos, 2014). Other simplified quasi-static methods (Andersen and Lauritzsen, 1988; Wang et al., 2005; Andresen et al., 2008) have also been extensively adopted, but do not reflect the cyclic degradation process of the soft clay and thus the undrained strength.

It remains a challenging task to develop a practical yet robust model with fewer parameters which addresses the influence of the cyclic strength degradation of soft ground on the stability of structures. Note that Wang et al. (2016) established an empirical degradation model based on the assumption that the undrained strength of soils decreases with the amplitude of cyclic-induced pore pressures. However, the influence of the damage and remolding of soft clay on the degradation of undrained strength was not considered. Therefore, in this paper we refine the previous degradation model to address cyclic damage-dependency using a damage parameter related to the accumulated plastic deviatoric strain to quantify the degree of damage and remolding of soft clay. The degradation model employs the post-cyclic undrained strength degradation coefficient, in terms of the cyclic stress ratio and the number of cycles, through the correlation between the maximum pore pressure and the undrained strength of soft clay. Based on the Tresca yield criterion, the model of undrained strength of soft clay was numerically implemented in the user interface USDFLD of ABAQUS, and applied to the numerical simulation of a caisson breakwater resting on a partially sand-filled soft clay seabed.

2 Damage-dependent degradation model of undrained strength of soft clay

Recent studies indicate that the undrained strength degradation of saturated clay during cyclic loading can be attributed to two mechanisms: the destruction of the soil fabric (Hu et al., 2012a) and the development of excess pore pressure (Mortezaie and Vucetic, 2013). Therefore, the degree of damage and remolding of soft clay can be quantified by a damage parameter related to the accumulated plastic deviatoric strain. The degradation of undrained strength due to the development of excess pore pressure can be evaluated by the correlation between the maximum excess pore pressure and the undrained strength of soft clay.

2.1 Damage parameter

According to previous studies (Liang and Ma, 1992; Hu et al., 2012b), a damage scalar parameter ω, which is related to the accumulative plastic deviatoric strain ε^{p}, can be expressed as

$$\omega = 1 - \mathrm{e}^{-\beta\varepsilon^{\mathrm{p}}}, \tag{1}$$

where β represents a positive parameter and controls the rate of damage accumulation.

Many cyclic loading tests on soft clay have shown that there is a threshold value of cyclic loading, below which the accumulated plastic deviatoric strain will reach a shakedown state (Zhou and Gong, 2001; Hu et al., 2012b; Cai et al., 2017; Guo et al., 2018). If the loading level exceeds the threshold value, the accumulated plastic deviatoric strain will increase sharply and cyclic failure will be triggered. Therefore, the following hyperbolic curve is adopted to express the accumulation of cyclic plastic deviatoric strain below the threshold value:

$$\varepsilon^{\mathrm{p}} = \frac{N}{AN + B}, \tag{2}$$

where A and B are fitting parameters, and by which we can guarantee a minimum residual sum of squares between test data and a fitting curve. N is the number of cycles. Substituting Eq. (2) into Eq. (1) yields

$$\omega = 1 - \mathrm{e}^{-\beta\varepsilon^{\mathrm{p}}} = 1 - \mathrm{e}^{-\beta\frac{N}{AN+B}}. \tag{3}$$

2.2 Degradation of undrained strength

During undrained cyclic shearing, the build-up of excess pore pressure in normally consolidated saturated soft clay leads to degradation of the undrained strength. In Fig. 1, *OP* represents the normal consolidation line (NCL), *PQ* represents the unloading line (UL), and CSL represents the critical state line. The cyclic degradation due to pore pressure generation denoted by *OQ* is considered to behave in a manner similar to the unloading segment *PQ* of the over-consolidated clay (Matsui et al., 1992; Yasuhara et al., 1992). The stress of soft clay reduces from the initial confining pressure p'_O to the current effective confining pressure p'_Q. This is regarded as the stress release of over-consolidated clay from p'_P to p'_Q. The reduction of undrained strength of over-consolidated clay depends on the horizontal distance between points P and Q, and the over-consolidated ratio can be defined as

$$\mathrm{OCR} = p'_P / p'_Q. \tag{4}$$

Similarly, the equivalent over-consolidated ratio is defined as

$$\mathrm{OCR}_{\mathrm{eq}} = p'_O / p'_Q. \tag{5}$$

Based on the equivalent over-consolidation concept (Yasuhara et al., 1992, Yasuhara, 1994), the undrained strength degradation of over-consolidated clay due to pore pressure generation can be expressed as

$$\frac{(c_{\mathrm{u}O})_{\mathrm{u}}}{(c_{\mathrm{u}O})_{\mathrm{nc}}} = \frac{(c_{\mathrm{u}Q})_{\mathrm{oc}}}{(c_{\mathrm{u}O})_{\mathrm{nc}}} = \mathrm{OCR}^{\Lambda_0 - 1} = (\mathrm{OCR}_{\mathrm{eq}})^{\frac{\Lambda_0}{1-c_{\mathrm{s}}/c_{\mathrm{c}}}-1}, \tag{6}$$

where $(c_{\mathrm{u}O})_{\mathrm{u}}$ represents the degradation of undrained strength of normally consolidated saturated soft clay due to pore pressure generation at point O, $(c_{\mathrm{u}O})_{\mathrm{nc}}$ is the static undrained strength of soft clay at point O, $(c_{\mathrm{u}Q})_{\mathrm{oc}}$ is the static undrained strength of over-consolidated saturated soft clay at point Q, Λ_0 is an experimental parameter, and c_{s} and c_{c} are swelling and compression indices, respectively.

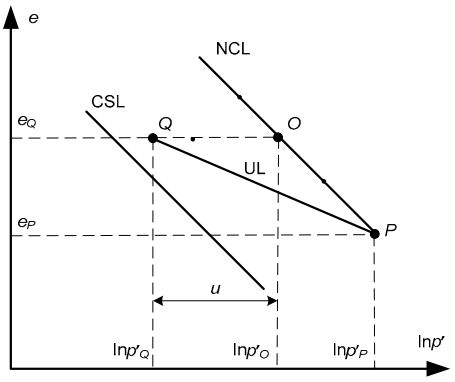

Fig. 1 NCL, UL, and CSL in *e*-ln*p′* plane

According to the principle of effective stress, Eq. (6) is rewritten in terms of the normalized excess pore pressure ratio u^*:

$$\delta_{\mathrm{u}} = \frac{(c_{\mathrm{u}O})_{\mathrm{u}}}{(c_{\mathrm{u}O})_{\mathrm{nc}}} = \left(\frac{1}{1-u/p'_O}\right)^{\frac{\Lambda_0}{1-c_{\mathrm{s}}/c_{\mathrm{c}}}-1} = (1-u^*)^m, \tag{7}$$

$$m = 1 - \frac{\Lambda_0}{1-c_{\mathrm{s}}/c_{\mathrm{c}}}, \tag{8}$$

where δ_{u} is the strength degradation coefficient due to pore pressure generation. The normalized excess pore pressure ratio u^* is defined as the ratio of the maximum pore pressure u to the confining pressure p', and m is a parameter related to Λ_0, c_{s}, and c_{c}.

It has been shown that there is a threshold value of cyclic loading amplitude which governs the pore pressure response of soils (Chen et al., 2005). When the stress amplitude is lower than the threshold value, the excess pore pressure increases gradually with the number of cycles, and then tends towards a steady state (Fig. 2). Therefore, a hyperbolic curve is adopted in this study to describe the development of the pore water pressure, as follows:

$$u^* = \frac{u}{p'} = \frac{N}{CN+D}, \tag{9}$$

where C and D are fitting parameters.

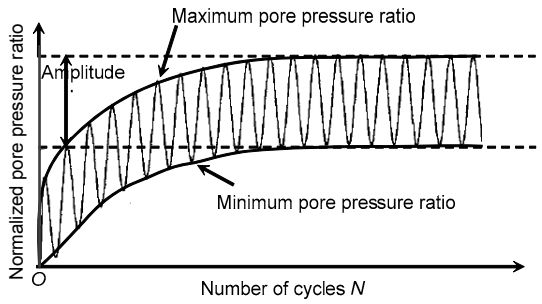

Fig. 2 Pore pressure development curve with cyclic number

Substituting Eq. (9) into Eq. (7) gives:

$$\delta_{\mathrm{u}}=\frac{(c_{\mathrm{u}})_{\mathrm{u}}}{(c_{\mathrm{u}})_{\mathrm{nc}}}=\left(1-\frac{N}{CN+D}\right)^{m}, \tag{10}$$

where $(c_{\mathrm{u}})_{\mathrm{u}}$ is the degraded undrained strength of normally consolidated saturated soft clay due to the pore pressure generation, and $(c_{\mathrm{u}})_{\mathrm{nc}}$ is the static undrained strength of soft clay.

2.3 Damage-dependent degradation model of undrained strength of soft clay

Based on Eqs. (1) and (7), the damage-dependent strength degradation model can be expressed as

$$\delta=\frac{(c_{\mathrm{u}})_{\mathrm{cy}}}{(c_{\mathrm{u}})_{\mathrm{nc}}}=(1-\alpha\omega)\delta_{\mathrm{u}}=\underbrace{(1-\alpha\omega)}_{\text{(i)}}\underbrace{(1-u^{*})^{m}}_{\text{(ii)}}, \tag{11}$$

where δ is the ratio of post-cyclic undrained strength $(c_{\mathrm{u}})_{\mathrm{cy}}$ to the static undrained strength $(c_{\mathrm{u}})_{\mathrm{nc}}$, and α is a positive model parameter that controls the degradation rate of undrained strength under cyclic loading. Note that Eq. (11) includes items (i) and (ii). Item (i) accounts for the strength degradation caused by the soil fabric and has an expression similar to that adopted by Liang and Ma (1992) and Hu et al. (2012b). Item (ii), δ_{u}, is used to consider the strength degradation induced by the pore pressure. Therefore, both the influence of the soil fabric and the accompanying pore pressure can be considered concurrently in Eq. (11).

By combining Eqs. (3), (10), and (11), we obtain the following equation for the strength degradation coefficient of soft clay:

$$\delta=\frac{(c_{\mathrm{u}})_{\mathrm{cy}}}{(c_{\mathrm{u}})_{\mathrm{nc}}}=\left(1-\alpha\left(1-\mathrm{e}^{-\beta\frac{N}{AN+B}}\right)\right)\left(1-\frac{N}{CN+D}\right)^{m}, \tag{12}$$

where parameters A and B are related to the accumulated plastic deviatoric strain of soft clay, and parameters C and D are related to the excess pore pressure and can be considered as a function of the cyclic stress ratio (CSR), defined as

$$\mathrm{CSR}=\sigma_{\mathrm{d}}/p', \tag{13}$$

where σ_{d} is the amplitude of the cyclic stress.

The damage-dependent degradation model of undrained strength of soft clay is then written as

$$\begin{aligned}\delta&=\frac{(c_{\mathrm{u}})_{\mathrm{cy}}}{(c_{\mathrm{u}})_{\mathrm{nc}}}=F(\mathrm{CSR},N)\\&=\left(1-\alpha\left(1-\mathrm{e}^{-\beta\frac{N}{A(\mathrm{CSR})N+B(\mathrm{CSR})}}\right)\right)\\&\quad\cdot\left(1-\frac{N}{C(\mathrm{CSR})N+D(\mathrm{CSR})}\right)^{m}.\end{aligned} \tag{14}$$

The developed model requires seven parameters (A, B, C, D, m, α, and β). As functions of the CSR, the parameters A, B, C, and D can be calibrated directly from cyclic triaxial (CTX) tests. m is an experimental parameter dependent on soil properties. Parameters α and β control the degree of damage and remolding of soft clay, and can be deduced through CTX tests by several trial and error attempts, as described in detail in Section 3.5.

3 Calibration of parameters

The muddy-silty clay near Yantai port, China was used to calibrate the model parameters using a series of static and CTX tests reported by Yang (2014).

3.1 Test procedures

All of the cyclic tests were conducted using a Global Digital System triaxial apparatus. Fully saturated samples of Yantai muddy-silty clay were first isotropically consolidated. Then a sinusoidal cyclic

stress with a cycle period of 8 s was immediately applied to the samples under undrained conditions. Four tests were performed to investigate the influence of the CSR on the degradation of undrained strength. The number of cycles was set to 1500, which is proven to be sufficient for the attainment of a constant value of excess pore pressure and axial strain. Another ten tests were conducted to evaluate the influence of the number of cycles, N, on the degradation of undrained strength, where CSR was set to 0.4, and the number of cycles, N, was set as 50, 100, 150, 200, 300, 500, 800, 1000, 1500 or 2000. The CSRs were all in the range of the threshold value that was determined as 0.5. The details of the CTX tests are summarized in Table 1.

Table 1 Details of the cyclic triaxial tests

Sample	Confining pressure (kPa)	Cyclic stress (kPa)	Cyclic stress ratio	Number of cycles
1–4	35	3.5, 7.0, 10.5, 14.0	0.1, 0.2, 0.3, 0.4	1500
5–14	35	14.0	0.4	50, 100, 150, 200, 300, 500, 800, 1000, 1500, 2000

3.2 Accumulated plastic deviatoric strain

Test data of the accumulated plastic deviatoric strain are shown in Fig. 3. By comparing the measured experimental data and the fitting curves by Eq. (2) with appropriate values of A and B, the accumulated plastic deviatoric strain can be expressed as follows:

$$\varepsilon^{\mathrm{p}}=\frac{N}{(-8.70\mathrm{CSR}+3.76)N+(918.17\mathrm{e}^{-9.36\mathrm{CSR}})}. \quad (15)$$

3.3 Maximum excess pore pressure

Similarly, proper values of C and D in Eq. (9) were selected to describe the development of the maximum excess pore pressure (Fig. 4). Eq. (16), which employs the normalized maximum excess pore pressure ratio u^*, was thus obtained as follows:

$$u^*=\frac{N}{(-8.55\mathrm{CSR}+5.01)N+(-5017.60\mathrm{CSR}+2435.06)}. \quad (16)$$

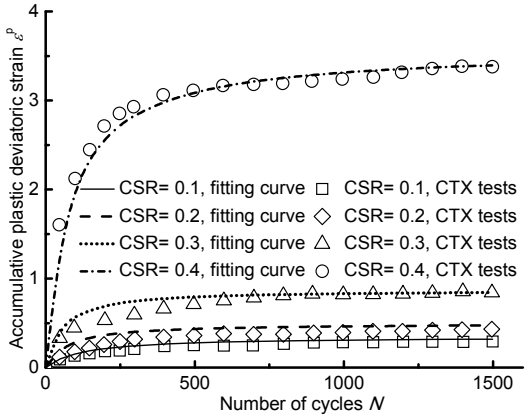

Fig. 3 CTX test results and fitting curves of accumulative plastic deviatoric strain

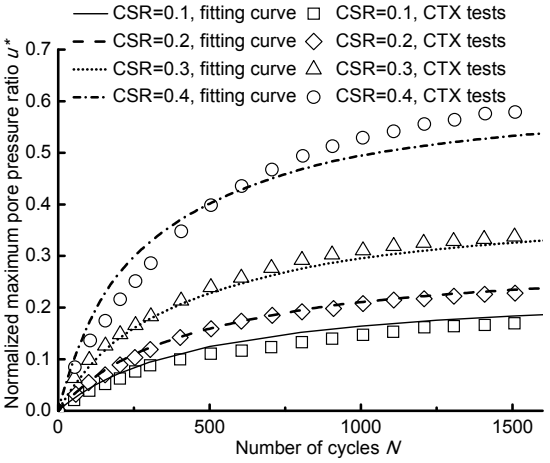

Fig. 4 CTX test results and fitting curves of normalized maximum pore pressure ratio

3.4 Values of experimental parameter *m*

To predict the undrained strength during cyclic loading using Eqs. (7) and (8), it is necessary to determine precisely the experimental parameter m in both equations. The experimental parameter Λ_0 of Yantai muddy-silty clay is 0.829, the swelling index c_s is 0.035, and the compression index c_c is 0.205 (Yang, 2014). Therefore, m can be calculated as 0.000 324 according to Eq. (8). However, parameter Λ_0 is found to vary significantly with the soil properties and testing conditions (Yasuhara, 1994). For example, values of Λ_0 are different for reconstituted and undisturbed soils, as well as for low and high plasticity soils. This could greatly affect the accuracy of m and cast undesired uncertainties on the model's reliability. Large deviations will emerge between the

undrained strength degradation of soft clay predicted by Eq. (8) and the CTX test data. Based on the review by Iizuka and Ohta (1987), the following empirical relations obtained by a statistical method (Ue et al., 1991) can be used to diminish errors:

$$c_s / c_c = 0.185 + 0.002 I_p, \tag{17}$$

$$\Lambda_0 / (1 - c_s / c_c) = 0.939 - 0.002 I_p, \tag{18}$$

$$m = 0.002 I_p + 0.061. \tag{19}$$

The above equations were derived from fitting the mean trends shown in Fig. 5, based on test data obtained from (Mayne, 1980). The values of both parameters c_s/c_c and Λ_0 are evaluated by the plastic index I_p that can be precisely measured in laboratory tests. The plastic index I_p of Yantai muddy-silty clay is 17.41, and the value of m is determined to be 0.096 by Eq. (19), which differs from the prediction of Eq. (8) by orders of magnitude.

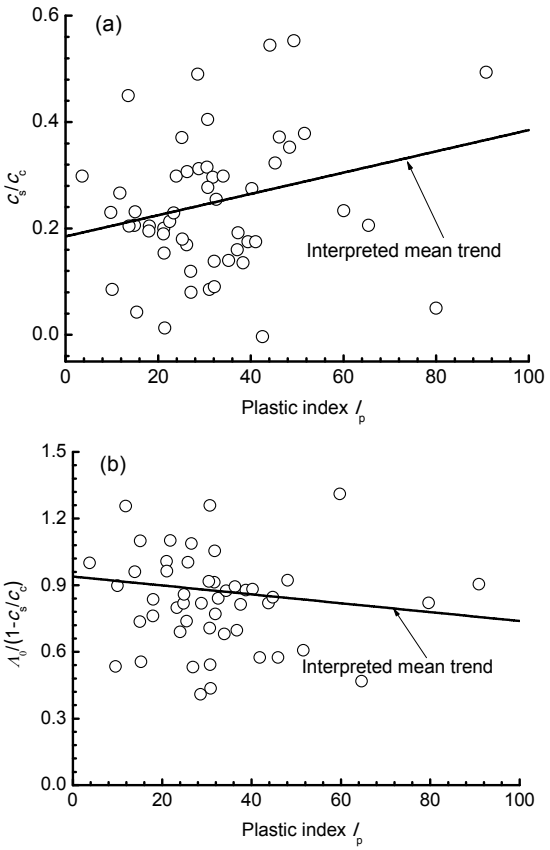

Fig. 5 Experimental fitting trends

(a) Relationships between c_s/c_c and I_p; (b) Relationships between $\Lambda_0/(1-c_s/c_c)$ and I_p

The parameter m quantifies the degree of strength degradation induced by the development of excess pore pressure. Fig. 6 shows that the strength degradation due to pore pressure development δ_u is hardly degraded using Eq. (8), while it is highly degraded using Eq. (19), and matches well with the test data of the undrained strength degradation after cyclic loading. The latter indicates that the development of excess pore pressure is the main cause of strength degradation rather than the destruction of the soil fabric below a threshold value of cyclic loading, which is in agreement with previous studies (Hu et al., 2012b; Yang, 2014). Therefore, Eq. (19) was used to evaluate the value of m in this study.

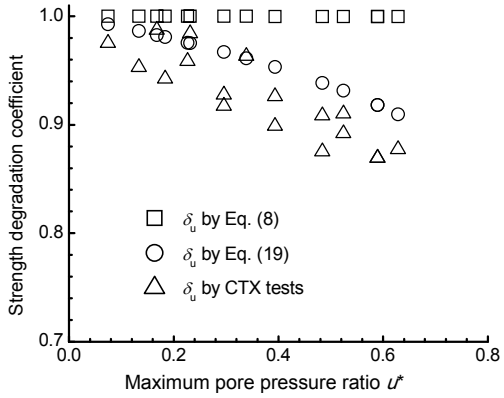

Fig. 6 Influence of various m values on strength degradation coefficients

3.5 Parameters α and β

Parameters α and β are related to the degree of damage and remolding of soft clay. The values of α and β are typically in the range of 0–5 for clay (Hu et al., 2012b). Considering the residual strength of the soil skeleton ($0<1-\alpha\omega<1$), values of α and β are suggested to vary in the ranges of 0–1.0 and 0–5.0, respectively.

Fig. 7 presents the influence of different combinations of α and β on post-cyclic strength degradation coefficients using Eq. (11). The undrained strength is degraded significantly with increasing values of α and β. Values of α and β can be obtained by the least square method as 0.9 and 1.5, respectively. Fig. 8 shows that the values of δ calculated by Eq. (11) fit the test data well. Values of δ are not single-valued with u^* because they are also affected by the damage

parameters that are different under various CSRs, indicating that the model can consider the effects of the soil fabric and the accumulation of pore pressures concurrently.

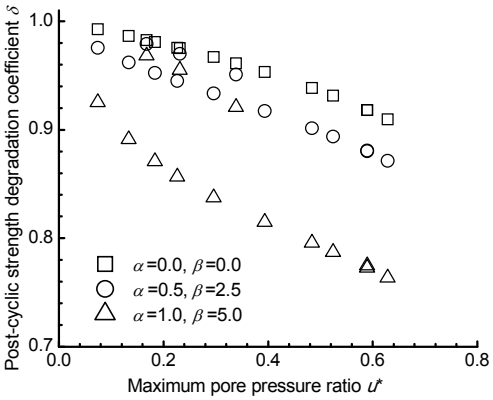

Fig. 7 Influence of α and β on post-cyclic strength degradation coefficients

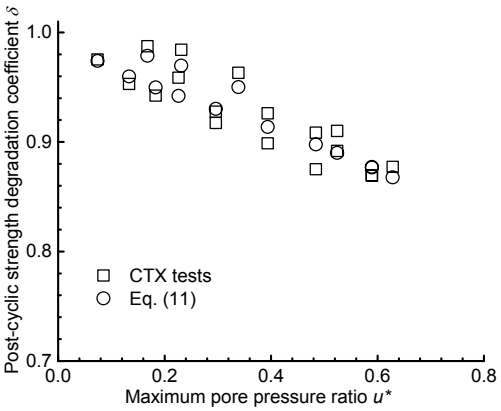

Fig. 8 Fitting points of Eq. (11) with test data when α is 0.9 and β is 1.5

4 Finite element analysis

4.1 Finite element implementation

The Tresca failure criterion is adopted to evaluate undrained capacity for monotonic or cyclic loading boundary value problems. To guarantee a good convergence, particularly in the calculation of the caisson-soft foundation problem, the following assumptions were made: (1) the soil will yield and fail quickly when the CSR reaches a threshold value; (2) there exists a lower limit value of the undrained strength ratio (Einav and Randolph, 2005; Xiao et al., 2016), and upper limit values of the accumulated plastic deviatoric strain and maximum excess pore pressure ratio (Wang et al., 2016). The following five key steps were used to implement the damage-dependent degradation model of undrained strength of soft clay with the Tresca failure criterion in the finite element program ABAQUS:

1. The confining pressure and stress in the major direction over the whole soil domain can be obtained from the field output and stored as two solution-dependent state variables S_0 and S_1, respectively.

2. Afterwards, the stress in the major direction of each soil element can be obtained with the GETVRM utility routine and stored as the third solution-dependent state variable S_2 in each increment. Thus, the CSR is obtained with the confining pressure S_0.

3. The undrained strength c_u for the Tresca model is defined as a field variable and calculated based on solution-dependent state variables in each increment by relating the Tresca model with the damage-dependent degradation model.

4. Update the Tresca model with the field variable $(c_u)_{cy}$: the plasticity strain is corrected and the stress of the soil is renewed based on the yield function, potential function, and flow rules of the Tresca model. The updated field variable $(c_u)_{cy}$ is employed as the initial condition in the next increment.

5. If the computing time reaches the designated time in the implicit dynamic step, then the computing process will be terminated. Otherwise, steps 2–4 are repeated and output variables are obtained.

A flow chart of the finite element implementation of the damage-dependent degradation model of soft clay based on the Tresca criterion is illustrated in Fig. 9.

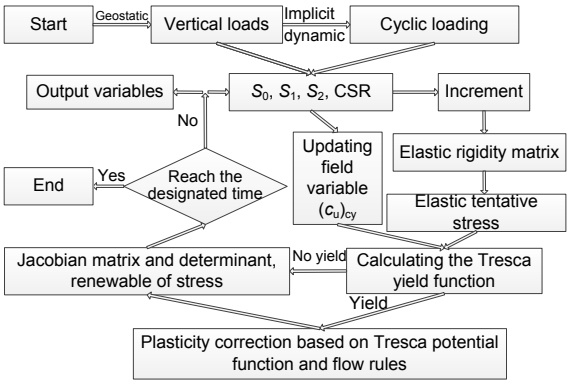

Fig. 9 Flow chart of finite element implementation

4.2 Numerical results and verification

A numerical calculation of a soil element using the damage-dependent degradation model of undrained strength was performed in ABAQUS to simulate the CTX tests. The performance of this model was verified by a comparison between the finite element method (FEM) results and CTX test data.

4.2.1 Damage parameter ω

Fig. 10 presents the finite element predictions of the damage parameter ω. Maximum values of ω increase with the number of cycles and tend to stabilize after a certain number of cycles. Maximum values of ω show a tendency to rise as the CSR increases.

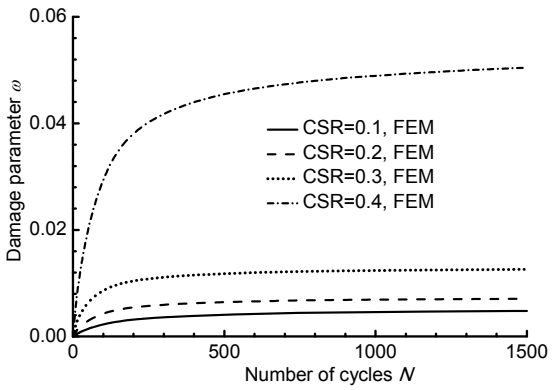

Fig. 10 Finite element predictions of damage parameter ω

4.2.2 Normalized maximum excess pore pressure ratio u^*

The finite element predictions of the normalized maximum excess pore pressure ratios u^* generally correspond to the test data in Fig. 11 for cyclic stress ratios of 0.1, 0.2, 0.3, and 0.4. The excess pore pressure increases with the increase of N and CSR, and generally remains unchanged after a certain number of cycles. Thus, the accuracy of the finite element development is confirmed.

4.2.3 Post-cyclic strength degradation of undrained strength of soft clay

Fig. 12 shows the finite element predictions and CTX test data of the post-cyclic undrained strength degradation coefficients of soft clay. The coefficients show a tendency to decline steeply at first and finally stabilize as N increases, while they decrease with increasing CSR. A generally acceptable correlation between the predictions by the finite element analysis and test data was achieved for CSRs of 0.1, 0.2, and 0.3 after 1500 number of cycles. The predictions of the post-cyclic undrained strength degradation coefficients were in good agreement with test data for CSR=0.4 with a series of numbers of cycles. Thus, the accuracy of the finite element development and the cyclic strength degradation model was affirmed.

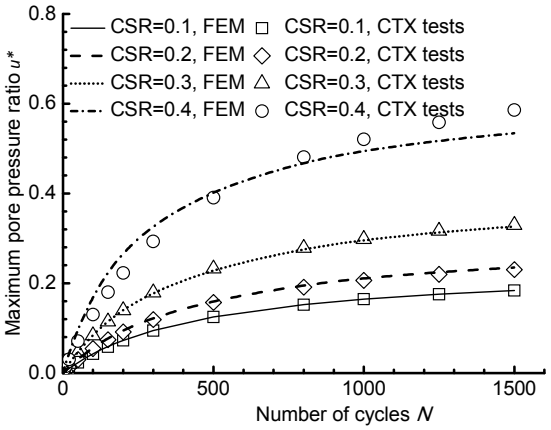

Fig. 11 Comparison between finite element predictions and cyclic triaxial test data

5 Numerical case study

The damage-dependent strength degradation model was applied to the numerical simulation of a caisson breakwater resting on a partially sand-filled soft clay seabed. The case study illustrates the applicability and efficiency of the model.

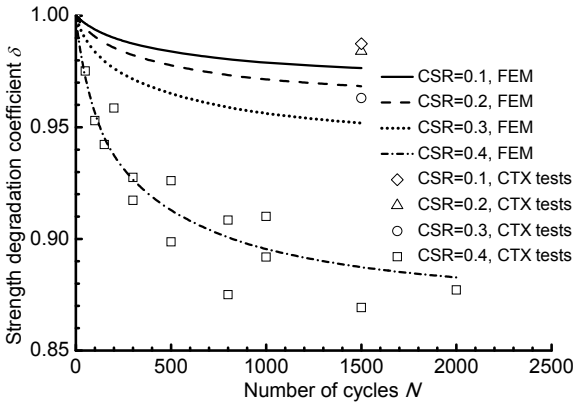

Fig. 12 Finite element predictions and cyclic triaxial test data of strength degradation coefficient δ

5.1 Case description

Fig. 13 presents the geometrical parameters of a caisson breakwater, which is 13 m high and 12 m wide with a 2-m-high parapet on the top, and constructed on a 5-m-high rubble bed. The depth of the soft layer is 20 m. After replacing the upper soft clay with a 7-m-deep sand layer, the depth of the remaining soft layer is 13 m. A sinusoidal wave cyclic loading was applied to the wave side of the caisson. The types of soil from the top to the bottom are: backfilled sand, soft clay, and medium sand. The main soil parameters are summarized in Fig. 13 and Table 2. In this study, the proposed undrained strength degradation model was used for the clay, and the Mohr-Columb model for the sand.

The finite element mesh is shown in Fig. 14. Plane strain elements were adopted to simulate the caisson, rubble bed, and soil. Also, nonlinear frictional contact was set up at the soil-structure interface. Fixed boundary conditions were adopted for the bottom of the numerical model, whereas the free boundary conditions and symmetry boundary conditions were adopted for the foundation surface and side surface, respectively. The boundaries were taken as impervious.

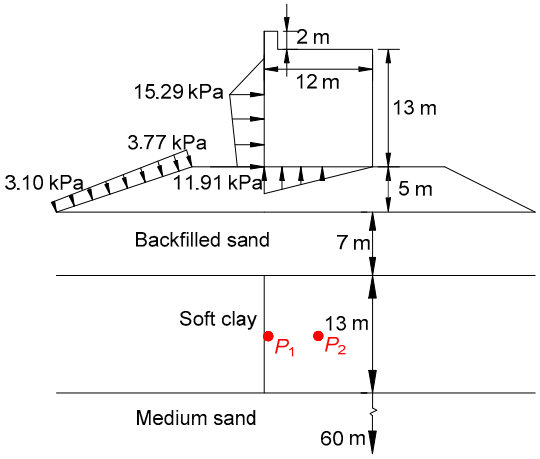

Fig. 13 Sketch of the numerical case study

5.2 Responses of the soft layer

In this section, the responses of the soft layer are presented in terms of the CSR, the maximum excess pore pressure, and the strength degradation of the foundation. The distribution of the CSR is first analyzed, after which the distributions of the maximum excess pore pressure and strength degradation of the foundation in relation to the cyclic stress and the number of cycles are investigated.

5.2.1 Cyclic stress distribution

Cyclic stress distribution of the soft layer is analyzed in terms of cyclic stress ratio in Fig. 15. As the distribution is hardly affected by the number of cycles when $N \geq 100$, only the distribution of $N=100$ is presented. It can be seen that the cyclic stress is mainly distributed at the bottom of the rubble bed, or more specifically, the distribution mode is bowl-shaped at the toes and right in the middle of the rubble bed due to the oscillating motion of the caisson under wave cyclic loading. Comparing with the cyclic stress in the middle of the rubble bed and the back side, the cyclic stress in the wave side (Fig. 14) is somewhat larger. Maximum values of cyclic stress are generated at the upper soft layer underneath the toe of the rubble bed.

5.2.2 Maximum excess pore pressure distribution

The maximum excess pore pressure distributions of the soft layer after 100 cycles and 500 cycles of wave loading are shown in Figs. 16a and 16b,

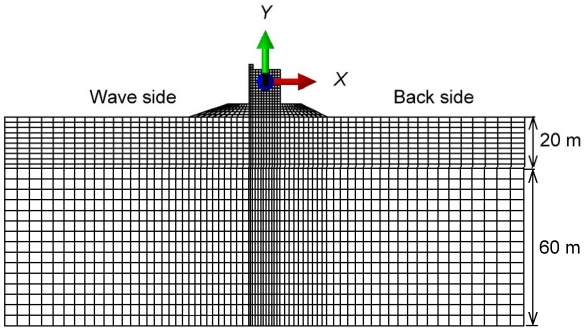

Fig. 14 Finite element discretization

Table 2 Soil parameters in the simulations

Soil layer	Young's modulus (MPa)	Effective unit weight (kN/m^3)	Friction angle (°)	Cohesion (kPa)	Vane shear strength (kPa)	Soil depth (m)
Backfilled sand	75	10.0	30.0	0.1	–	7
Soft clay	15	7.9	16.2	10.2	30.92	13
Medium sand	100	10.0	31.6	0.1	–	60

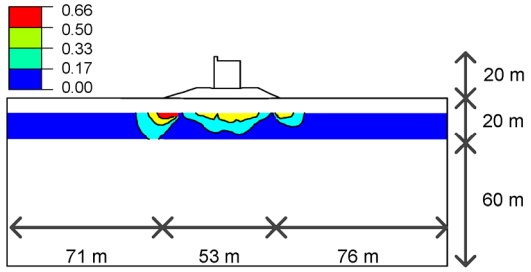

Fig. 15 Cyclic stress ratio of soft layer

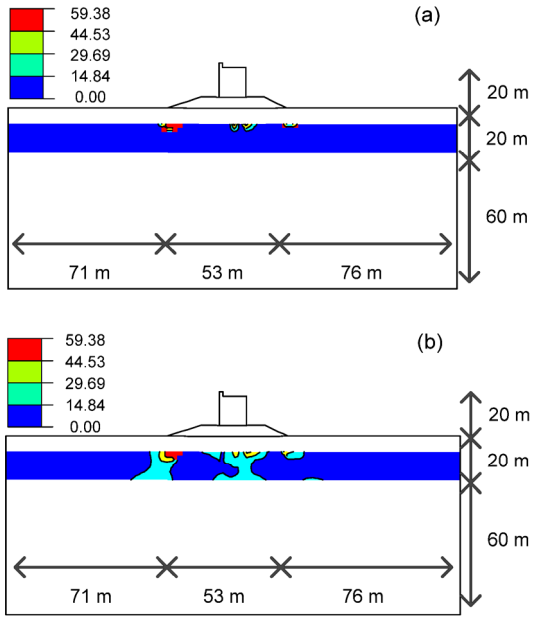

Fig. 16 Maximum excess pore pressure distributions of soft layer after 100 (a) and 500 (b) cycles of wave loading (unit: kPa)

respectively. The generation of maximum excess pore pressure was concentrated mainly at the toes and in the middle of the rubble bed, roughly in agreement with the distribution of the cyclic stress. Maximum excess pore pressure reached a peak in the upper soft layer underneath the toe of the rubble bed. However, some differences are apparent between cyclic stress areas and maximum excess pore pressure areas after 500 cycles. This is because the cyclic stress areas are presented in terms of the CSR which considers the influence of the confining pressure. Furthermore, the areas of excess pore pressure were significantly affected by the number of cycles, and were greater after 500 cycles than after 100 cycles. Numerical results show that maximum excess pore pressure is influenced by both the cyclic stress and the number of cycles.

The excess pore pressure time series at two typical points, P_1 and P_2, are shown in Fig. 17. The locations of these two points (Fig. 13) are underneath the front toe and in the center of the caisson, respectively, in the middle of the soft layer (13.5 m below the seabed surface). Excess pore pressure can be divided into the oscillating pore pressure and the residual pore pressure, as observed in previous study (Wang et al., 2014). The maximum excess pore pressure increased continuously with the number of cycles and reached 16 kPa after 500 cycles.

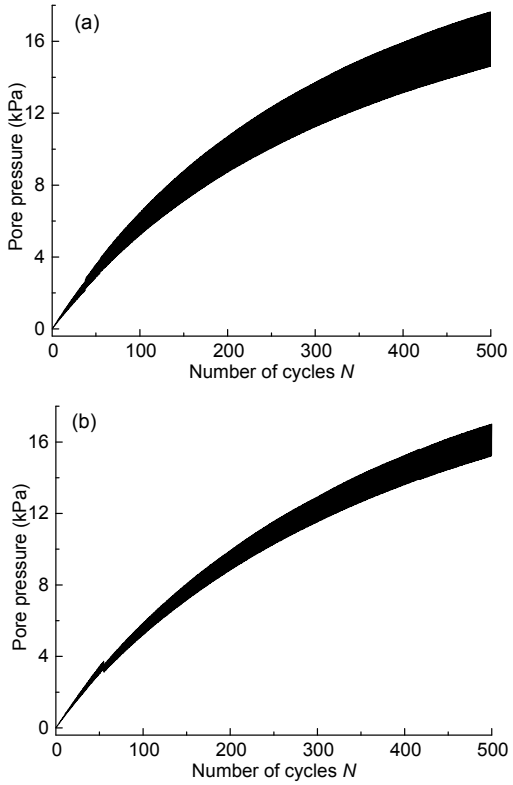

Fig. 17 Excess pore pressure time series at two typical points P_1 (a) and P_2 (b)

5.2.3 Strength degradation distribution

The degraded areas where the strength degradation coefficients were less than 0.84 were concentrated at the toes and in the middle of the rubble foundation in the upper soft layer, corresponding to the areas of cyclic stress (Figs. 18a and 18b). However, an effect of the number of cycles was not discernible due to the small size of the areas that were degraded.

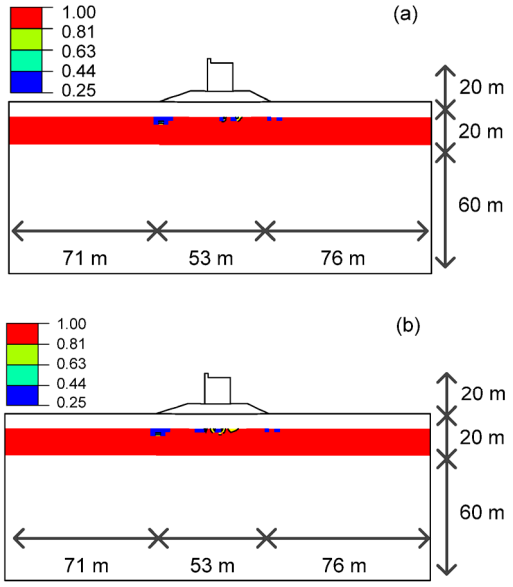

Fig. 18 Strength degradation coefficients of soft layer after 100 (a) and 500 (b) cycles of wave loading

6 Conclusions

This paper introduces a degradation model to describe the damage-dependent behavior of soft clay under cyclic loading conditions. In the model, a damage parameter that quantifies the degree of damage and remolding of soft clay was first related to the accumulated plastic deviatoric strain. The correlation was then established between the maximum pore pressure and the undrained strength of soft clay to employ the post-cyclic undrained strength degradation coefficient in terms of the CSR and the number of cycles. Model parameters were calibrated by a series of static and CTX tests of muddy-silty clay near Yantai port. Based on the Tresca yield criterion, the damage-dependent strength degradation model of undrained strength of soft clay was numerically implemented in the user subroutine of ABAQUS. Some conclusions can be drawn as follows:

1. The numerical response of a soil element using the damage-dependent strength degradation model of undrained strength was implemented in ABAQUS to simulate the response of a soil element in CTX tests below a threshold value of CSR. Results showed that the maximum values of the damage variable ω and the maximum excess pore pressure ratio u^* increased with the number of cycles N and stabilized after a certain number of cycles, and increased with the CSR. The undrained strength degradation coefficients of soft clay showed a tendency to fall at first then finally reached a stable status with increasing N, and decreased with increasing CSR.

2. Finite element predictions of the maximum excess pore pressure and the undrained strength degradation coefficients generally matched the test data well, confirming the accuracy of the finite element development and the damage-dependent strength degradation model.

3. The damage-dependent strength degradation model was applied to the numerical simulation of a caisson breakwater resting on a partially sand-filled soft clay seabed. Results showed that the responses of the soft layer were mainly distributed at the toes and in the middle of the rubble bed. There was an effect of the number of cycles on the maximum excess pore pressure, but not on the cyclic stress and undrained strength degradation. The proposed model of the damage-dependent strength degradation of undrained soft clay is practical and robust, and provides an efficient method for analyzing the interaction between offshore structures and soft soil foundations.

References

Allotey N, El Naggar MH, 2008. A consistent soil fatigue framework based on the number of equivalent cycles. *Geotechnical and Geological Engineering*, 26(1):65-77. https://doi.org/10.1007/s10706-007-9147-2

Andersen KH, Lauritzsen R, 1988. Bearing capacity for foundations with cyclic loads. *Journal of Geotechnical Engineering*, 114(5):540-555. https://doi.org/10.1061/(ASCE)0733-9410(1988)114:5(540)

Andresen L, Jostad HP, Andersen KH, 2008. Finite element analyses in offshore foundation design. Proceedings of the 12th International Conference of International Association for Computer Methods and Advances in Geomechanics, p.3247-3262.

Cai YQ, Guo L, Jardine RJ, et al., 2017. Stress-strain response of soft clay to traffic loading. *Geotechnique*, 67(5):446-451. https://doi.org/10.1680/jgeot.15.P.224

Chen W, Randolph MF, 2007. Uplift capacity of suction caissons under sustained and cyclic loading in soft clay. *Journal of Geotechnical and Geoenvironmental Engineering*, 133(11):1352-1363. https://doi.org/10.1061/(ASCE)1090-0241(2007)133:11(1352)

Chen YM, Lai XH, Ye YC, 2005. Wave-induced pore water

pressure in marine cohesive soils. *Acta Oceanologica Sinica*, 24(4):138-145.

Einav I, Randolph MF, 2005. Combining upper bound and strain path methods for evaluating penetration resistance. *International Journal for Numerical Methods in Engineering*, 63(14):1991-2016. https://doi.org/10.1002/nme.1350

Gerolymos N, Gazetas G, 2006. Development of Winkler model for static and dynamic response of caisson foundations with soil and interface nonlinearities. *Soil Dynamics and Earthquake Engineering*, 26(5):363-376. https://doi.org/10.1016/j.soildyn.2005.12.002

Guo L, Cai YQ, Jardine RJ, et al., 2018. Undrained behaviour of intact soft clay under cyclic paths that match vehicle loading conditions. *Canadian Geotechnical Journal*, 55(1):90-106. https://doi.org/10.1139/cgj-2016-0636

Hu C, Liu HX, 2015. A new bounding-surface plasticity model for cyclic behaviors of saturated clay. *Communications in Nonlinear Science and Numerical Simulation*, 22(1-3): 101-119. https://doi.org/10.1016/j.cnsns.2014.10.023

Hu C, Liu HX, Huang W, 2012a. Anisotropic bounding-surface plasticity model for the cyclic shakedown and degradation of saturated clay. *Computers and Geotechnics*, 44:34-47. https://doi.org/10.1016/j.compgeo.2012.03.009

Hu C, Liu HX, Huang W, 2012b. Damage-dependent bounding surface model for cyclic degradation of saturated clay. *Rock and Soil Mechanics*, 33(2):459-466 (in Chinese). https://doi.org/10.3969/j.issn.1000-7598.2012.02.023

Huang MS, Liu YH, Sheng DC, 2011. Simulation of yielding and stress-stain behavior of Shanghai soft clay. *Computers and Geotechnics*, 38(3):341-353. https://doi.org/10.1016/j.compgeo.2010.12.005

Iizuka A, Ohta H, 1987. A determination procedure of input parameters in elasto-viscoplastic finite element analysis. *Soils and Foundations*, 27(3):71-87. https://doi.org/10.3208/sandf1972.27.3_71

Karapiperis K, Gerolymos N, 2014. Combined loading of caisson foundations in cohesive soil: finite element versus Winkler modeling. *Computers and Geotechnics*, 56:100-120. https://doi.org/10.1016/j.compgeo.2013.11.006

Kudella M, Oumeraci H, DeGroot MB, et al., 2006. Large-scale experiments on pore pressure generation underneath a caisson breakwater. *Journal of Waterway, Port, Coastal, and Ocean Engineering*, 132(4):310-324. https://doi.org/10.1061/(asce)0733-950X(2006)132:4(310)

Lee SR, Oh S, 1995. An anisotropic hardening constitutive model based on generalized isotropic hardening rule for modelling clay behaviour. *International Journal for Numerical and Analytical Methods in Geomechanics*, 19(10):683-703. https://doi.org/10.1002/nag.1610191003

Liang RY, Ma FG, 1992. Anisotropic plasticity model for undrained cyclic behavior of clays. I: Theory. *Journal of Geotechnical Engineering*, 118(2):229-245. https://doi.org/10.1061/(asce)0733-9410(1992)118:2(229)

Liyanapathirana DS, 2009. Arbitrary Lagrangian Eulerian based finite element analysis of cone penetration in soft clay. *Computers and Geotechnics*, 36(5):851-860. https://doi.org/10.1016/j.compgeo.2009.01.006

Matsui T, Bahr M, Abe N, 1992. Estimation of shear characteristics degradation and stress-strain relationship of saturated days after cyclic loading. *Soils and Foundations*, 32(1):161-172. https://doi.org/10.3208/sandf1972.32.161

Mayne PW, 1980. Cam-clay predications of undrained strength. *Journal of the Geotechnical Engineering Division*, 106(11):1219-1242. https://doi.org/10.1016/0148-9062(81)91013-5

Mortezaie AR, Vucetic M, 2013. Effect of frequency and vertical stress on cyclic degradation and pore water pressure in clay in the NGI simple shear device. *Journal of Geotechnical and Geoenvironmental Engineering*, 139(10):1727-1737. https://doi.org/10.1061/(ASCE)GT.1943-5606.0000922

Oumeraci H, 1994. Review and analysis of vertical breakwater failures-lessons learned. *Coastal Engineering*, 22(1-2): 3-29. https://doi.org/10.1016/0378-3839(94)90046-9

Ue S, Yasuhara K, Fujiwara H, 1991. Influence of consolidation period on undrained strength of clays. *Ground and Construct*, 9(1):51-62 (in Japanese).

Ulker MBC, Rahman MS, Guddati MN, 2010. Wave-induced dynamic response and instability of seabed around caisson breakwater. *Ocean Engineering*, 37(17-18):1522-1545. https://doi.org/10.1016/j.oceaneng.2010.09.004

Wang H, Liu HJ, Zhang MS, 2014. Pore pressure response of seabed in standing waves and its mechanism. *Coastal Engineering*, 91:213-219. https://doi.org/10.1016/j.coastaleng.2014.06.005

Wang JH, Li C, Moran K, 2005. Cyclic undrained behavior of soft clays and cyclic bearing capacity of a single bucket foundation. Proceedings of the 15th International Offshore and Polar Engineering Conference, p.392-399.

Wang YZ, Yan Z, Wang YC, 2016. Numerical analyses of caisson breakwaters on soft foundations under wave cyclic loading. *China Ocean Engineering*, 30(1):1-18. https://doi.org/10.1007/s13344-016-0001-2

Xiao Z, Tian YH, Gourvenec S, 2016. A practical method to evaluate failure envelopes of shallow foundations considering soil strain softening and rate effects. *Applied Ocean Research*, 59:395-407. https://doi.org/10.1016/j.apor.2016.06.015

Yan SW, Liu R, Fan QJ, et al., 2005. Stability of the guiding dike in Yangtze Estuary under the wave load. *China Ocean Engineering*, 19(4):659-670. https://doi.org/10.3321/j.issn:0890-5487.2005.04.011

Yang PB, 2014. Experimental Study on the Strength Weakening Character of Muddy-silty Clay under Cyclic Dynamic Loading. MS Thesis, Tianjin University, Tianjin, China (in Chinese).

Yasuhara K, 1994. Postcyclic undrained strength for cohesive soils. *Journal of Geotechnical Engineering*, 120(11): 1961-1979. https://doi.org/10.1061/(ASCE)0733-9410(1994)120:11(1961)

Yasuhara K, Hirao K, Hyde A, 1992. Effects of cyclic loading on undrained strength and compressibility of clay. *Soils and Foundations*, 32(1):100-116. https://doi.org/10.3208/sandf1972.32.100

Zhou J, Gong XN, 2001. Strain degradation of saturated clay under cyclic loading. *Canadian Geotechnical Journal*, 38(1):208-212. https://doi.org/10.1139/cgj-38-1-208

Zhou J, Yan JJ, Liu ZY, et al., 2014. Undrained anisotropy and non-coaxial behavior of clayey soil under principal stress rotation. *Journal of Zhejiang University-SCIENCE A (Applied Physics & Engineering)*, 15(4):241-254. https://doi.org/10.1631/jzus.A1300277

中文概要

题　目： 饱和软黏土不排水强度弱化模型及其在沉箱式防波堤的应用分析

目　的： 本文旨在建立简单实用的饱和软黏土不排水强度损伤弱化模型，应用于波浪循环荷载作用下沉箱式防波堤与软土地基相互作用的非线性数值计算，为解决防波堤软土强度弱化计算问题提供有效途径。

创新点： 1. 基于不排水强度循环损伤弱化机理，得到软黏土不排水强度随循环荷载作用次数和应力水平的变化规律；2. 结合 Tresca 屈服准则进行数值开发，应用于波浪循环荷载作用下沉箱式防波堤与软土地基相互作用的数值计算。

方　法： 1. 引入累积塑性变形相关的损伤变量表征土体结构性的损伤和重塑对软黏土不排水强度弱化的影响（公式（3）和（11））；2. 建立软黏土不排水强度随循环荷载作用次数和应力水平变化的损伤弱化模型（公式（14））；3. 结合 Tresca 屈服准则，实现软黏土不排水强度损伤弱化的数值计算过程（图 9）；4. 针对烟台软黏土动三轴试验数据进行分析，对模型及其数值开发过程进行验证（图 11 和 12）；5. 将模型应用到软土地基上沉箱式防波堤数值运算，分析软土地基响应，验证模型的有效性（图 15~18）。

结　论： 1. 在临界循环应力比以下，损伤变量和归一化最大孔压比随循环荷载作用次数的增加逐渐增大，并趋于稳定；随循环应力比增大逐渐增大。循环后不排水强度折减系数随着循环荷载作用次数和循环应力比的增加而减小。2. 有限元数值开发过程是正确的，不排水强度损伤弱化模型是合理的。3. 该模型简单实用，可应用于波浪等循环荷载作用下沉箱式防波堤与软土地基相互作用的非线性数值计算，且能模拟循环荷载下软土地基的孔隙水压力增长以及不排水强度弱化等响应。软土地基的响应主要分布在基床两趾及正下方的软土层上部。

关键词： 饱和软黏土；不排水强度；循环弱化模型；损伤；数值模拟